commodities

MDPI

Article

An Econometric and Time Series Analysis of the USTC Depeg's Impact on the LUNA Classic Price Crash During Spring 2022's Crypto Market Turmoil

Papa Ousseynou Diop

Laboratoire d'Économie Dionysien (LED), University Paris 8, 93526 Saint-Denis, France; papa-ousseynou.diop@anciens.univ-paris1.fr

Abstract: The cryptocurrency market is characterized by extreme volatility, with events such as the Terra-LUNA crash of 2022 raising significant questions about the resilience of algorithmic stablecoins. This paper investigates the collapse of LUNA Classic during the USTC depeg, focusing on the role of trading volumes and collateral assets like Bitcoin in amplifying the price crash. Using a Vector Logistic Smooth Transition AutoRegressive (VLSTAR) model, we analyze daily data from October 2020 to November 2022 to uncover how exogenous volumes influenced LUNA's price trajectory during the crisis. Our findings reveal that high trading volumes, particularly during regime two (the post-depeg period), significantly exacerbated the price decline, validating the impact of large-scale liquidations on LUNA's price path. Additionally, Bitcoin volumes played a critical role in destabilizing the system, confirming that the liquidity of underlying collateral assets is pivotal in maintaining price stability. These insights contribute to understanding the systemic vulnerabilities in algorithmic stablecoins and offer implications for future stablecoin design and risk management strategies. They are relevant for investors, policymakers, and researchers seeking to be aware of market volatility and prevent future crises in stablecoin ecosystems.

Keywords: LUNA; stablecoin; TerraUSD; depeg; smooth transition VAR; Bitcoin; cryptocurrency market crash

Citation: Diop, P.O. An Econometric and Time Series Analysis of the USTC Depeg's Impact on the LUNA Classic Price Crash During Spring 2022's Crypto Market Turmoil. *Commodities* **2024**, *3*, 431–459. https://doi.org/10.3390/commodities3040024

Academic Editor: Jungho Baek

Received: 19 September 2024
Revised: 21 November 2024
Accepted: 28 November 2024
Published: 1 December 2024

1. Introduction

The cryptocurrency market has witnessed several high-profile crashes over the past decade [1], each revealing unique vulnerabilities within digital assets [2]. Is it a Ponzi scheme, a speculative event similar to "tulip mania", or the outcome of a technological shift in decentralized finance that might lead central banks to develop a digital currency? Researchers will tell. However, the Terra-LUNA crash of 2022 stands out due to its systemic impact on the market [3] and its roots in the collapse of an algorithmic stablecoin, TerraUSD (USTC) [4]. Unlike traditional stablecoins, which are typically backed by reserves [5], USTC was designed to maintain its dollar peg through an algorithmic arbitrage mechanism with its sister token, LUNA [6]. When USTC lost its peg in May 2022 [7], this mechanism failed to stabilize it [8], leading to a self-reinforcing downward spiral that ultimately wiped out over USD 40 billion in market value [9]. This event exposed inherent risks in algorithmic stablecoin designs [2], raising important questions for investors and policymakers regarding liquidity [10], transparency [11], and systemic risk in digital asset ecosystems [4].

The Terra-LUNA collapse differs from previous cryptocurrency downturns, which were often driven by external shocks, such as regulatory uncertainty (i.e., the 2018 Bitcoin crash [12]) driven by regulatory uncertainty) or speculative bubbles [8]. Instead, this crash was a result of an internal mechanism failure within the stablecoin's algorithmic framework, marking it as an unprecedented case of systemic risk originating from within the digital asset itself [13]. Given the vulnerabilities exposed by the Terra-LUNA crash, this study addresses the following research question:

"How did the USTC depeg influence the price crash of LUNA, and what role did trading volumes and collateral assets like Bitcoin play in amplifying the crisis?"

We examine the mechanisms of this collapse by applying a Vector Logistic Smooth Transition AutoRegressive (VLSTAR) model to analyze daily data from October 2020 to November 2022, and we investigate the dynamic interactions between USTC's depeg and LUNA's price crash, offering insights into the nonlinear dependencies that characterize algorithmic stablecoin failures. The choice of time period in the analysis is guided by the fact that the Terra Luna crash occurred in 2022, and the key events (the USTC depeg and LUNA price collapse) are already captured in the dataset up to November 2022. Extending the data beyond this period would not add value to understanding the crash since the asset is no longer actively traded in a way that is meaningful to my study. And also, after Terra Luna's collapse, the coin's market activity became insignificant or irrelevant to the broader crypto ecosystem. Updating the dataset would not capture meaningful market behavior, as the post-2022 period reflects the aftermath of a failed asset, rather than any significant price or volume dynamics.

While the Terra-LUNA collapse is largely attributed to the failure of its internal algorithmic stabilizing mechanism, some alternative viewpoints suggest that external market conditions played a significant role in exacerbating the crisis [4]. One hypothesis is that the crash was primarily driven by internal algorithmic issues—specifically, the design flaw in Terra's arbitrage mechanism, which could not maintain USTC's dollar peg under high sell-off pressure [6]. This internal instability triggered a feedback loop, where the collapse of the stablecoin led to a rapid devaluation of its collateral, LUNA, further intensifying the sell-off and eroding investor confidence [14]. An alternative hypothesis emphasizes the impact of external market conditions, including broader instability in the cryptocurrency market and liquidity constraints, which may have intensified the effects of the internal algorithmic failure [15]. Proponents of this view argue that the "crypto winter" of 2022 created a context of high volatility and reduced liquidity, making Terra's algorithmic design more vulnerable than it might have been under stable market conditions [16]. According to this perspective, external shocks, such as rising interest rates and macroeconomic instability, could have precipitated or accelerated the failure of USTC's peg.

By examining the role of both internal and external factors, this study acknowledges the complexity of the Terra-LUNA collapse and seeks to clarify the mechanisms by which the USTC depeg specifically impacted LUNA's price trajectory while accounting for the broader market context.

Despite the growing literature on cryptocurrency volatility and stablecoins, there remains a research gap regarding the specific risks posed by algorithmic stablecoins like USTC. Prior studies have largely focused on traditional stablecoins or other cryptocurrencies, often attributing price instability to external shocks. This study aims to address this gap by analyzing how endogenous mechanisms, such as algorithmic stabilization failures, can amplify price volatility and create systemic risks within the cryptocurrency market. For the statistical analysis, we use a vector smooth transition regression model, the VLSTAR model, as proposed by [17], which enhances our understanding of forecasting dynamics. This study extends recent work on linear model selection and adequacy tests for univariate smooth transition regression models to a multivariate context. Using these tests, the study examines the nonlinear forecasting abilities of the conference board's composite index of leading indicators in predicting both output growth and business cycle phases of the US economy in real time. Similarly, ref. [18] utilized a nonlinear vector autoregression model that incorporated variables such as output, prices, and money supply to analyze the asymmetric effects of monetary policy. The estimation strategy used in this study is consistent with various structural macroeconomic models.

Our analysis using the *VLSTAR model* captures these nonlinear dynamics, revealing that high trading volumes, particularly those involving Bitcoin, significantly exacerbated

LUNA's price decline in the post-depeg period. This finding underscores the critical role of collateral liquidity in maintaining stablecoin prices, especially during market downturns.

These insights hold relevance for *investors*, who need to understand the unique risks associated with algorithmic stablecoins, and for *policymakers*, who face the challenge of developing regulatory frameworks that address the liquidity and transparency risks posed by such assets. By highlighting how algorithmic mechanisms within stablecoins can amplify market instability, this study provides practical implications for risk management and regulatory oversight in digital asset markets.

The remainder of this paper is structured as follows: Section 2 presents the data and methods used in the analysis, including the application of econometric and time series models tailored to capture volatility dynamics in the Terra-LUNA market. Section 3 discusses the empirical results, followed by Section 4, which addresses robustness checks and further model testing. Section 5 concludes with a discussion of key findings, policy implications, and potential directions for future research.

2. LUNA Classic Univariate Analysis

2.1. Quantitative Analysis

CUSUM is a sequential analysis technique used to detect significant structural changes in time series data. It works by calculating the cumulative sum of deviations from a reference value (e.g., the mean or target value of the series). In this study, CUSUM is applied to LUNA's price data to identify structural breaks in its price dynamics before and after the crash. The steps involved include the following:

1. Establishing a Baseline: a reference mean or target price for LUNA is calculated based on historical data prior to the crash.
2. Computing Deviations: at each time point, the difference between the observed price and the reference value is computed.
3. Cumulative Summation: these deviations are accumulated over time to track significant trends or abrupt shifts.

CUSUM is particularly valuable in this context because it visualizes the timing and magnitude of price deviations that align with critical market events, such as the start of the crash. This makes it a powerful tool for diagnosing the moment when market conditions deteriorated and helps identify early warning signs of instability. According to [19], the CUSUM procedure signaled that the shift occurred the first time:

$$S_n = \sum_{i=1}^{n} \log \frac{f_B(x_i)}{f_G(x_i)} - \min_{k \leqslant n} \sum_{i=1}^{k} \log \frac{f_B(x_i)}{f_G(x_i)} > L,$$

where f_B and f_G are densities corresponding to F_B and F_G, respectively, L is a constant that determines the operating characteristics of the procedure, and log means the natural logarithm. As with the usual sequential probability ratio test, the constant L does not depend on n. The statistic S_n can be calculated recursively in the following way:

$$S_n = \max\left(S_{n-1} + \log \frac{f_B(x_n)}{f_G(x_n)}, 0\right).$$

We may "rescale" the equation by dividing the log of $f_B(x_n)/f_G(x_n)$ and L by the same constant. Rescaling results in an equivalent procedure that is easier to use. The initial value for CUSUM, S_0, is some number between 0 and L. The careful choice of S_0 gives a CUSUM with improved properties. The value of the preceding formula is that for several common distributions, having been reduced to a very simple procedure.

Figure 1 presents the price dynamics of LUNA, showcasing its trajectory before, during, and after the crash. The economic significance of this visualization lies in identifying the stages of market behavior:

1. Pre-Crash Stability: reflects market confidence in LUNA as part of the Terra ecosystem, driven by its role in maintaining USTC's peg.
2. Crash Onset: highlights the initial depeg of USTC and its immediate effects on LUNA's value, signaling a loss of confidence among investors.
3. Post-Crash Recovery or Decline: provides insights into market responses, such as whether speculative investors attempted to "buy the dip" or if confidence was entirely eroded.

From an economic perspective, this figure illustrates how price movements reflect broader systemic vulnerabilities, such as a dependence on algorithmic stabilization and susceptibility to panic-driven sell-offs.

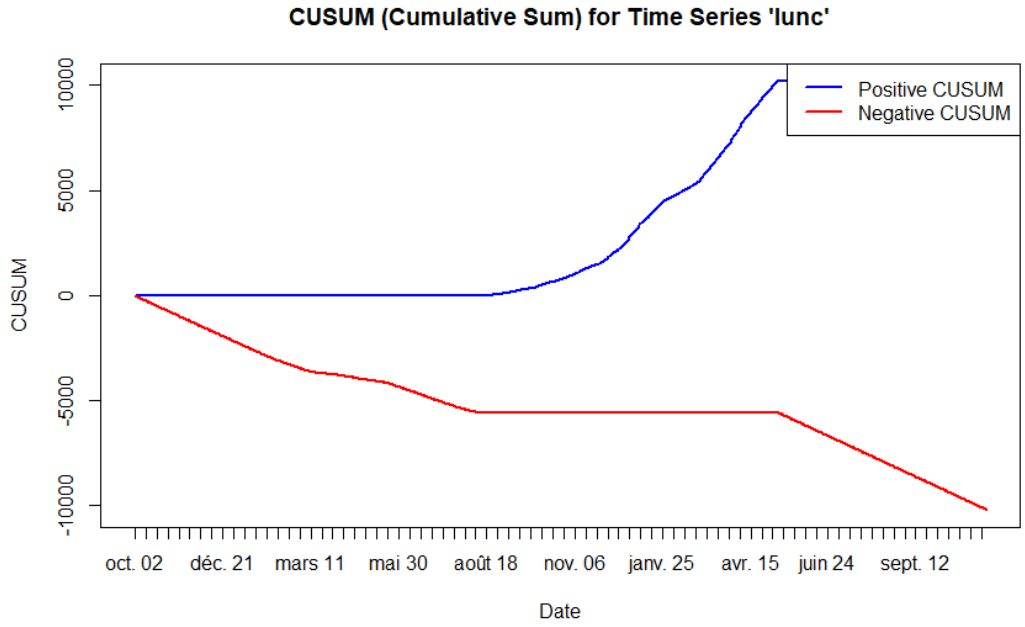

Figure 1. Cusum of LUNC.

According to [20], time series can be decomposed into cyclical trend and seasonal decompositions (see [21] for a review). Trend decomposition is used to break down LUNA's price movements into three main components:

1. Trend Component: captures the long-term directional movement of LUNA's price, reflecting its fundamental value over time.
2. Cyclical Component: represents short- to medium-term fluctuations caused by market sentiment, speculation, or external shocks.
3. Residual Noise: accounts for random, unexplained variations in the price data.

The method used for decomposition in this analysis involves a smoothing technique (e.g., moving averages or the Hodrick–Prescott filter) to isolate these components. By separating the trend and cycle, the analysis highlights the shift in LUNA's market behavior—from stability to extreme volatility—providing clear evidence of the crash's timing and underlying drivers.

Figure 2 shows changes in trading volumes, which are critical for understanding market sentiment:

1. High Volumes During Crash: a surge in trading volumes during the crash period indicates panic selling, as investors rapidly liquidate positions.
2. Volatility After the Crash: fluctuations in trading volumes post crash may indicate speculative trading or attempts to stabilize the market through coordinated buying.

The relationship between price and trading volume provides valuable economic insights into liquidity dynamics and investor behavior during periods of market stress. For

instance, a simultaneous price decline and high trading volume during the crash indicates heavy liquidation, reflecting a systemic crisis of confidence.

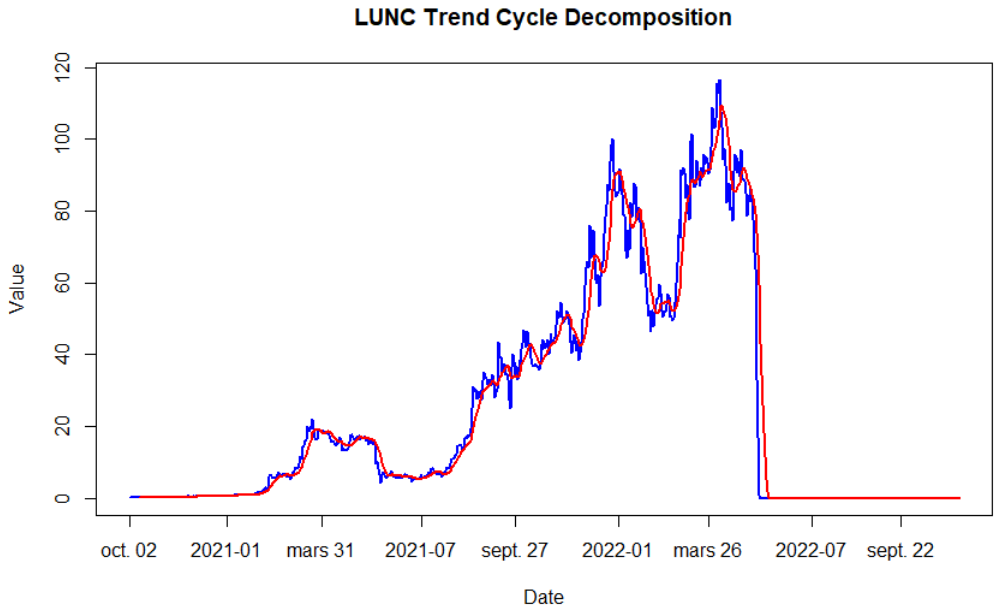

Figure 2. Decomposition of LUNC.

Table 1 presents descriptive statistics such as the mean, standard deviation, minimum, and maximum values for LUNA and USTC prices and trading volumes. The standard deviation highlights the extreme price and volume fluctuations characteristic of cryptocurrency markets. For LUNA and USTC, high volatility underscores the inherent risks of algorithmic stablecoins. The minimum and maximum values illustrate the dramatic swings during the crash, emphasizing the impact of the systemic failure on investor wealth. Comparing LUNA and USTC statistics reveals the interplay between the stablecoin's depeg and the associated collateral asset's collapse. For example, if USTC's average price deviates significantly from its USD peg, it signals prolonged instability, with repercussions for LUNA's value.

Table 1. Descriptive statistics for LUNC.

LUNC	Open	High	Low	Close	Adj Close	Volume	Returns	LogRet
count	1100.00	1100.00	1100.00	1100.00	1100.00	1100.00	1100.00	1100.00
mean	17.23	18.16	16.31	17.23	17.23	684.11	0.01	−0.01
std	28.53	29.86	27.18	28.52	28.52	1218.69	0.15	0.24
min	0.00	0.00	0.00	0.00	0.00	0.17	−1.00	−5.55
10%	0.00	0.00	0.00	0.00	0.00	3.13	−0.08	−0.08
25%	0.19	0.20	0.19	0.19	0.19	6.96	−0.04	−0.04
50%	0.43	0.47	0.39	0.43	0.43	168.74	0.00	0.00
75%	18.76	19.68	18.12	18.79	18.79	860.40	0.04	0.04
90%	67.34	73.36	62.71	67.37	67.37	2142.97	0.10	0.09
max	116.42	119.18	114.11	116.41	116.41	15,924.39	3.50	1.50
var	813.77	891.57	738.97	813.55	813.55	1,485,204.11	0.02	0.06

2.2. Trading Analysis

Traders employ machine learning models to monitor the trajectory of LUNA contract prices, utilizing technical indicators such as exponential moving averages (EMAs). This indicator is commonly utilized in trading practices to evaluate the price trends of assets. Exponential moving averages (EMAs) are significant in volatile markets like cryptocurrencies because they give greater weight to recent data points, making them highly responsive

to sudden price changes. This characteristic makes EMAs ideal for capturing short- to medium-term trends in volatile markets, where price movements can shift rapidly. By smoothing out noise and emphasizing the most recent price movements, EMAs help traders identify potential entry and exit points with greater accuracy, which is crucial in markets like crypto, where prices can fluctuate dramatically within hours.

For example, during the LUNA crash, EMAs would have quickly highlighted the accelerating downward trend in prices, signaling a bearish market sentiment and providing insights into the timing and severity of the collapse. An EMA is a type of moving average that assigns greater importance to recent data points, enabling traders to gauge how an asset's price has fluctuated over a specific time frame.

According to [22], the EWMA is very easily plotted and may be graphed simultaneously with the data appearing on a Shewhart chart. The EWMA is best plotted one time position ahead of the most recent observation. A later discussion will show the EWMA may be viewed as the forecast for the next observation, but that need not bother us here. Our immediate purpose is only to plot the statistic. The EWMA equals the present predicted value plus λ times the present observed error of prediction. Thus,

$$\begin{aligned} \text{EWMA} &= \hat{y}_{t+1} = \hat{y}_t + \lambda e_t \\ &= \hat{y}_t + \lambda(y_t - \hat{y}_t) \end{aligned}$$

where

$$\begin{aligned} \hat{y}_{t+1} &= \text{ predicted value at time } t+1 \text{ (the new EWMA);} \\ y_t &= \text{ observed value at time } t; \\ \hat{y}_t &= \text{ predicted value at time } t \text{ (the old EWMA);} \\ e_t = y_t - \hat{y}_t &= \text{ observed error at time } t. \end{aligned}$$

λ is a constant $(0 < \lambda < 1)$ that determines the depth of memory of the EWMA. The equation can be written as

$$\hat{y}_{i+1} = \lambda y_i + (1-\lambda)\hat{y}_i.$$

The 10-day EMA is highly responsive to recent price changes because it assigns greater weight to the most recent prices. In volatile markets like cryptocurrencies, where rapid price fluctuations occur, this sensitivity makes it a valuable tool for detecting early changes in market trends. The 10-day EMA is represented by the red line in Figure 3. This line indicates an upward trend in the LUNC price from 11 January 2021 to 12 May 2021. Since the EMA indicator for shorter periods is more sensitive to price changes, it is a useful tool for investors seeking to enter or exit trades.

On-balance volume (OBV) is an indicator that predicts changes in stock price by using volume flow (see [23] for a technical review). It reflects market sentiment by tracking the flow of volume into and out of an asset. OBV adds the trading volume on up days and subtracts it on down days, creating a cumulative measure that shows whether buying or selling pressure dominates.

During the LUNA crash, OBV highlighted the significant increase in selling pressure as panic set in among investors. A sharp decline in OBV indicated a loss of confidence and the massive liquidation of positions, illustrating the broader market sentiment. The divergence between price and OBV (e.g., a declining OBV alongside collapsing prices) underscored the overwhelming sell-off driven by fear and distrust in the algorithmic stablecoin's ability to maintain its peg. The formula for OBV is

$$\text{OBV} = \text{OBV}_{\text{prev}} + \begin{cases} \text{volume}, & \text{if close} > \text{close}_{\text{prev}} \\ 0, & \text{if close} = \text{close}_{\text{prev}} \\ -\text{volume}, & \text{if close} < \text{close}_{\text{prev}} \end{cases}$$

where OBV = current on-balance volume level; OBV_{prev} = previous on-balance volume level; and volume = latest trading volume amount.

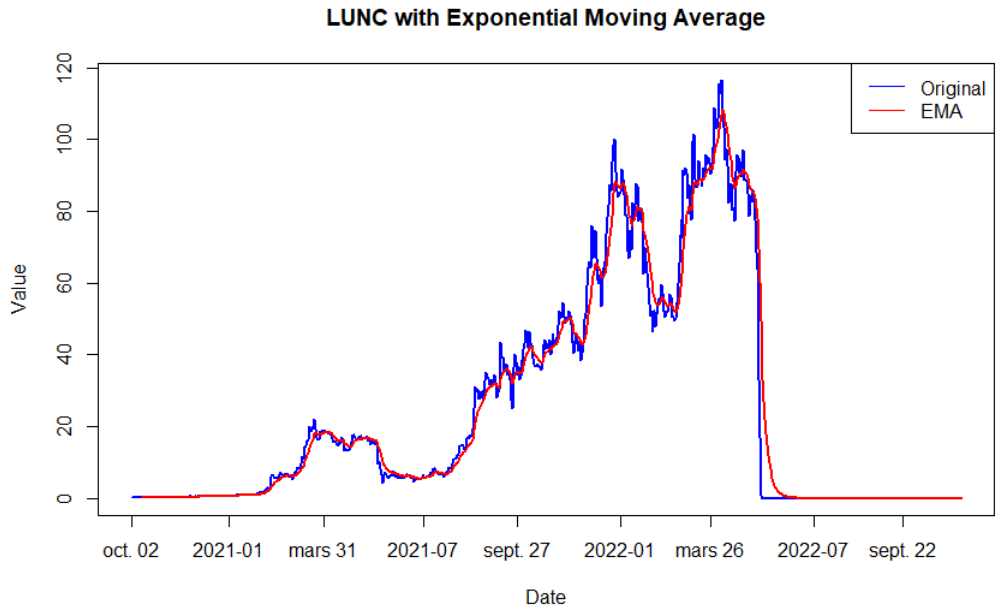

Figure 3. EMA of LUNC.

Figure 4 visualizes the cumulative buying and selling pressure based on trading volume, offering a sentiment-driven perspective of market behavior. We note a rise in the price of LUNC on 11 January 2022 and mid-May that indicates that investors were accumulating LUNA, reflecting confidence in its stability and future growth. Then, as is seen with a peak in the volumes exchanged, with the depeg of the USTC to date, the LUNC suddenly loses all of its value, which is gradually cancelled. This corresponds to widespread sell-offs, driven by fear and a loss of trust in the Terra ecosystem, demonstrating the intensity of panic selling and the liquidity drain from the market. By this way, the OBV captures the systemic risk of algorithmic stablecoins by showing how quickly liquidity can drain during a crisis.

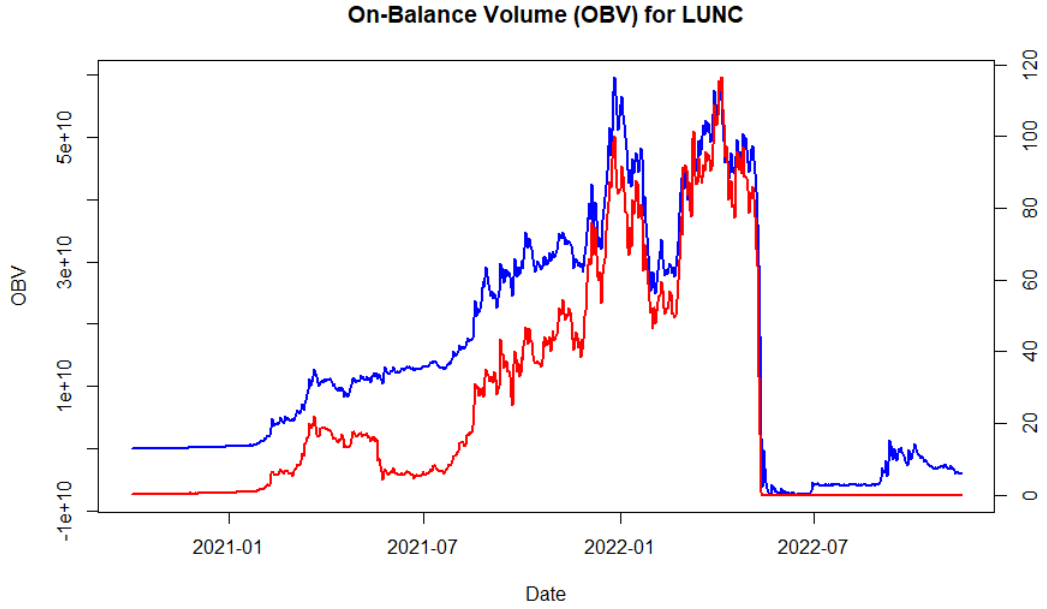

Figure 4. OBV of LUNC.

According to [24], the volume-weighted average price is one of the most common benchmarks used for judging the execution quality of a trading strategy by institutional investors, pension funds, or mutual funds. The volume-weighted average price (VWAP) is

an indicator used by professional traders. It is calculated by totaling the dollars traded for every transaction (price multiplied by the volume) and then dividing by the total shares traded. The VWAP is calculated using the following formula:

$$\text{VWAP}_t = \frac{\sum_{i=1}^{t}(P_i \times V_i)}{\sum_{i=1}^{t} V_i}$$

where P_i is the LUNC price at time i, V_i is the LUNC volume at time i, t represents the current time period, and the summation runs from 1 to t, the length of the time series.

In the VWAP, the numerator is conveniently the cumulative sum of the product of price and volume, whereas the denominator is the cumulative sum of the volume. This gives the VWAP at each time t, which can be used to analyze price movements weighted by volume, offering a better understanding of price trends when large volume spikes occur.

In Figure 5, the VWAP reaches a climax in May 2022, the moment from which it falls with its depeg. The VWAP represents the average price of LUNC, weighted by trading volume, and offers insights into fair value during market turmoil. It provides a baseline for assessing whether LUNC was trading above or below its average price during the crash. A price below the VWAP during the collapse confirms intense selling pressure. Its peaking in May 2022 aligns with the peak in trading activity during USTC's depeg, marking the climax of panic-driven liquidations.

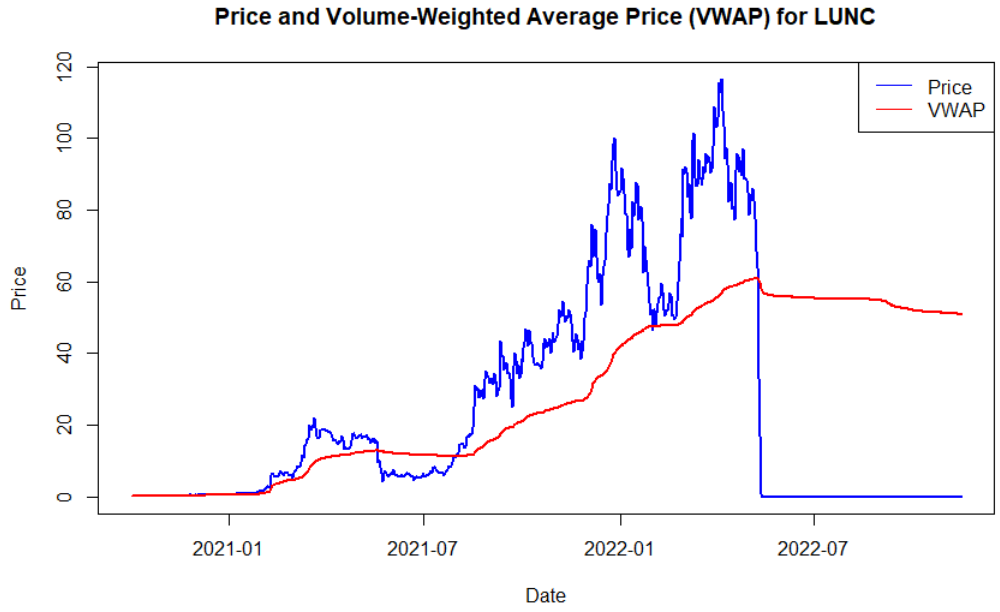

Figure 5. VWAP of LUNC.

2.3. Prediction

Recurrent neural networks (RNNs) are a type of neural network that retain a memory of what it has already been processed and thus can learn from previous iterations during its training. RNNs are particularly suited for cryptocurrency predictions due to their ability to model sequential dependencies in time series data. Cryptocurrencies exhibit high volatility and nonlinear dynamics, where price trends often depend on past behaviors. RNNs, with their feedback loops, can "remember" these temporal relationships, making them effective for capturing patterns in historical data and predicting future price movements. The functioning recurrent neural network (RNN) model used in this paper is described thoroughly in [25].

Recall that RNNs are a class of neural networks that allow previous outputs to be used as inputs while having hidden states. Formally, for each timestep t, the activation $a^{<t>}$ and the output $y^{<t>}$ are expressed as follows:

$$a^{<t>} = g_1\left(W_{aa}a^{<t-1>} + W_{ax}x^{<t>} + b_a\right) \quad \text{and } y^{<t>} = g_2\left(W_{ya}a^{<t>} + b_y\right)$$

where $W_{ax}, W_{aa}, W_{ya}, b_a$, and b_y are coefficients that are shared temporally and g_1, g_2 activation functions.

k-nearest neighbors (k-NN), on the other hand, is a simpler yet robust algorithm that performs well for cryptocurrency price trends by leveraging historical patterns. Its instance-based approach allows it to handle nonlinear data distributions by finding similarities between new data points and historical observations. This makes k-NN an effective baseline for a comparison against more complex models like the RNN.

As for Table 2, we evaluate predictive performance metrics of both recurrent neural networks (RNN) and k-NN for LUNC price movements. Here, the RNN displays a mean squared error (MSE) of 399.1785, a root mean squared error (RMSE) of 19.9795, and values indicating moderate accuracy in trend tracking, particularly from early 2021 to the significant crash in 2022. The k-NN model shows lower error rates (MSE: 268.13, RMSE: 16.3746), suggesting better robustness in price prediction for this period. However, this paper notes that while both models effectively capture trend shifts, k-NN excels in short-term accuracy by leveraging historical patterns in volatile crypto markets like LUNC.

Table 2. RNN and k-NN forecast statistics for LUNC.

LUNC	MSE	RMSE	Mean Per-Class Error	Log-Loss
RNN	399.17845	19.97945		
k-NN	2.6813×10^2	1.637461×10^1	1.727558×10^6	

For a test point, $\mathbf{x}$, consider the set of the k nearest neighbors of $\mathbf{x}$ as $S_\mathbf{x}$. Formally $S_\mathbf{x}$ is defined as $S_\mathbf{x} \subseteq D$ s.t. $|S_\mathbf{x}| = k$ and $\forall(\mathbf{x}', y') \in D \backslash S_\mathbf{x}$,

$$\text{dist}(\mathbf{x}, \mathbf{x}') \geq \max_{(\mathbf{x}'', \mathbf{y}'') \in S_\mathbf{x}} \text{dist}(\mathbf{x}, \mathbf{x}''),$$

(i.e., every point in D but not in $S_\mathbf{x}$ is at least as far away from $\mathbf{x}$ as the furthest point in $S_\mathbf{x}$). We can then define the classifier $h()$ as a function returning the most common label in $S_\mathbf{x}$:

$$h(\mathbf{x}) = \text{mode}(\{y'' : (\mathbf{x}'', y'') \in S_\mathbf{x}\}),$$

where mode $(\cdot)$ means to select the label of the highest occurrence.

The k-nearest neighbor classifier fundamentally relies on a distance metric. The better the metric reflects label similarity, the better the classifier will be. The most common choice is the Minkowski distance

$$\text{dist}(\mathbf{x}, \mathbf{z}) = \left(\sum_{r=1}^{d} |x_r - z_r|^p\right)^{1/p}$$

Ref. [26] provide an overview of the k-NN unsupervised machine learning algorithm. As for Table 2, the same comment applies for k-NN.

In brief, RNNs excel in capturing temporal relationships in sequential data, while k-NN serves as a strong benchmark for nonlinear pattern detection without requiring complex training. Using these models together provides a balance between simplicity (k-NN) and the ability to model dynamic dependencies (RNN). However, if computational resources permit, LSTMs (Long Short-Term Memory) and GRUs (Gated Recurrent Units) might outperform RNNs for handling longer-term dependencies due to their ability to mitigate the vanishing gradient problem.

3. USTC Univariate Analysis

3.1. Quantitative Analysis

Figure 6 illustrates the decomposition of USTC's price movements into long-term trends, cyclical components, and residual noise. The steady value of USTC before May 2022 reflects its algorithmic peg to the US dollar, maintaining stability as intended. However, the sharp decline post May 2022 signifies a collapse of confidence in the algorithmic mechanism underlying the peg. This decomposition highlights two economic aspects:

1. Long-term stability pre-collapse: indicates the system's perceived reliability, attracting deposits and fostering investor trust in a low-volatility environment.
2. Systemic failure post depeg: the sharp decline reflects the structural fragility of algorithmic stablecoins, where small shocks (e.g., large withdrawals or a loss of confidence) can lead to catastrophic, self-reinforcing feedback loops.

This decomposition helps isolate these dynamics, offering a clearer understanding of the transition from stability to collapse and the underlying economic behaviors driving these changes.

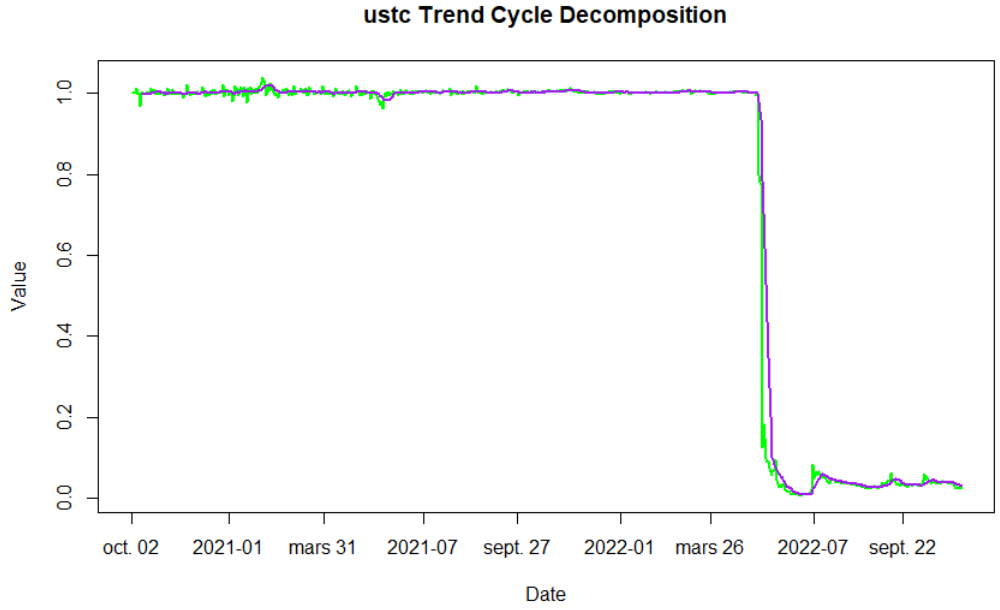

Figure 6. Decomposition of USTC.

CUSUM tracks cumulative changes in USTC's value, providing a statistical method to detect shifts in price dynamics. In Figure 7, the flat line pre-collapse indicates stability, while the steep drop during the depeg event reflects a sudden structural break in USTC's price. Economically, this sharp shift captures the following:

1. Investor Panic: the rapid decline in the CUSUM line aligns with widespread liquidations as trust in the stablecoin evaporates.
2. Market Feedback Loops: the feedback between USTC's depegging and LUNA's hyperinflation caused a cascading collapse in both assets, as reflected in the CUSUM line's dramatic change.

The CUSUM visualization emphasizes the systemic vulnerabilities in algorithmic stablecoins and the speed at which trust can unravel, highlighting the economic risks of inadequate stabilization mechanisms.

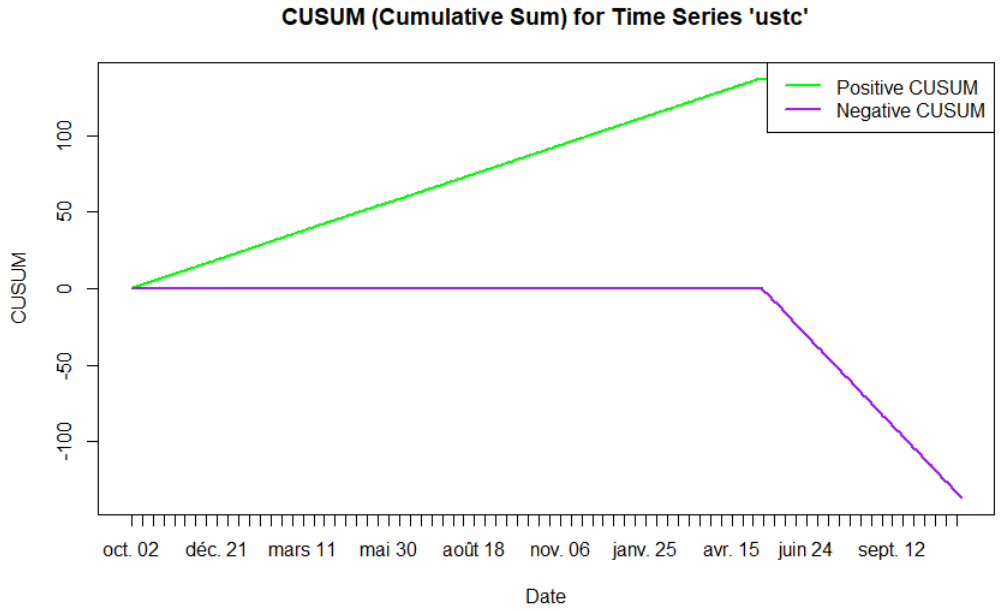

Figure 7. CUSUM of USTC.

3.2. Trading Analysis

The EMA highlights the speed at which market sentiment deteriorates in response to structural weaknesses. It serves as a visual tool for identifying critical turning points in market confidence, particularly in algorithmically governed systems.

Regarding the exponential moving average analysis, Figure 8 shows us that the 10-day EMA line tracks USTC's stock price movements, providing a smoothed, short-term trend line. This figure is critical for understanding the dynamics before and during the USTC depeg event. During the pre-depeg event, the EMA closely follows USTC's stable price around USD 1, reflecting the success of the algorithmic peg mechanism during normal market conditions. During the crash in 2022's Spring, the 10-day EMA sharply trends downward, lagging slightly behind the actual price but effectively signaling a breakdown in stability. The two series equalize to zero afterwards. This rapid decline reflects the algorithm's inability to maintain the peg under stress, driven by investor panic and large-scale liquidations.

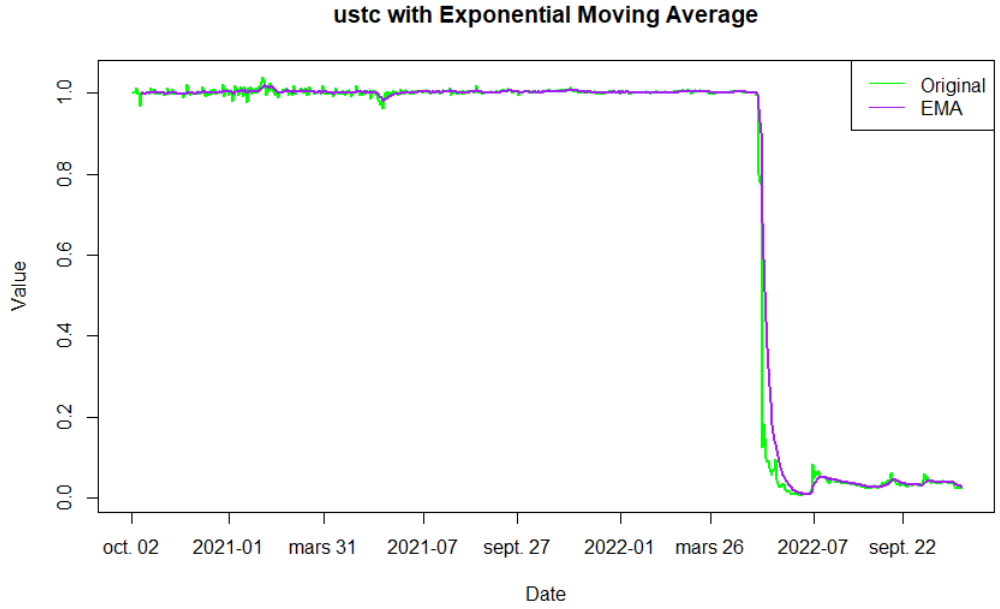

Figure 8. EMA of USTC.

The OBV tracks cumulative volume changes, offering a sentiment-driven perspective on market behavior. Regarding on-balance volume analysis, we note in Figure 9 the constancy of the price of USTC between 11 January 2022 and mid-May (the date of its depeg), indicating balanced buying and selling activity as the USTC price remains pegged. Then, it suddenly loses all of its value with its depeg, highlighting widespread liquidation. The steep drop reflects panic selling as investors lost confidence in USTC's ability to maintain its peg.

The decline in OBV signals a systemic loss of trust, where investor behavior drives a feedback loop of falling prices and heightened liquidation. The OBV's trends capture the scale and intensity of the sell-off.

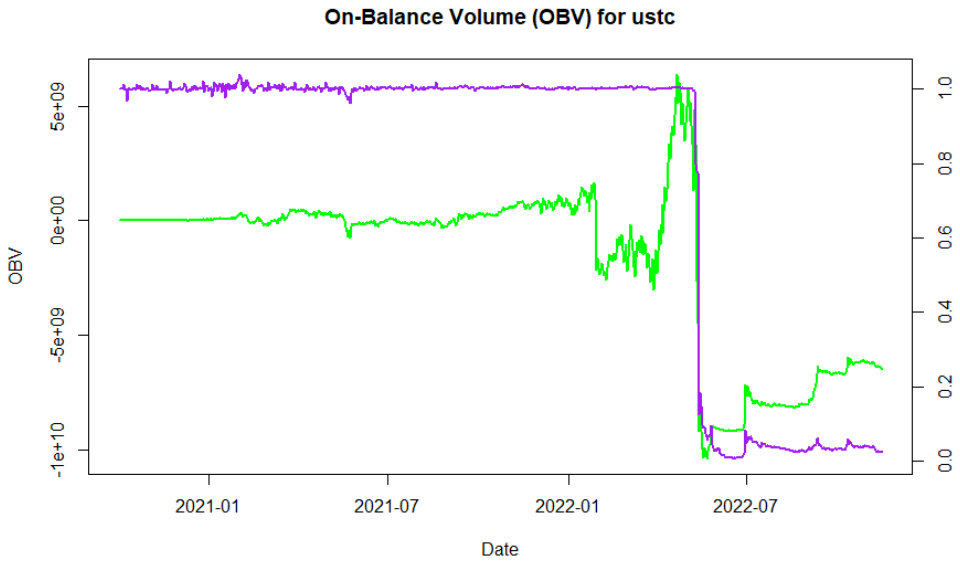

Figure 9. OBV of USTC.

The VWAP reflects the average price of USTC, weighted by trading volume, providing insights into the fair value during the depeg crisis. Regarding the volume-Weighted average price analysis, in Figure 10 the USTC price is stable and equates to USD since November 2020 mirroring the stable price of USTC and reflecting the algorithmic peg's success during normal conditions. Then in May 2022 a significant divergence occurs as USTC's price falls far below the VWAP. This indicates intense selling pressure and the erosion of fair value, as panic trading activity dominates.

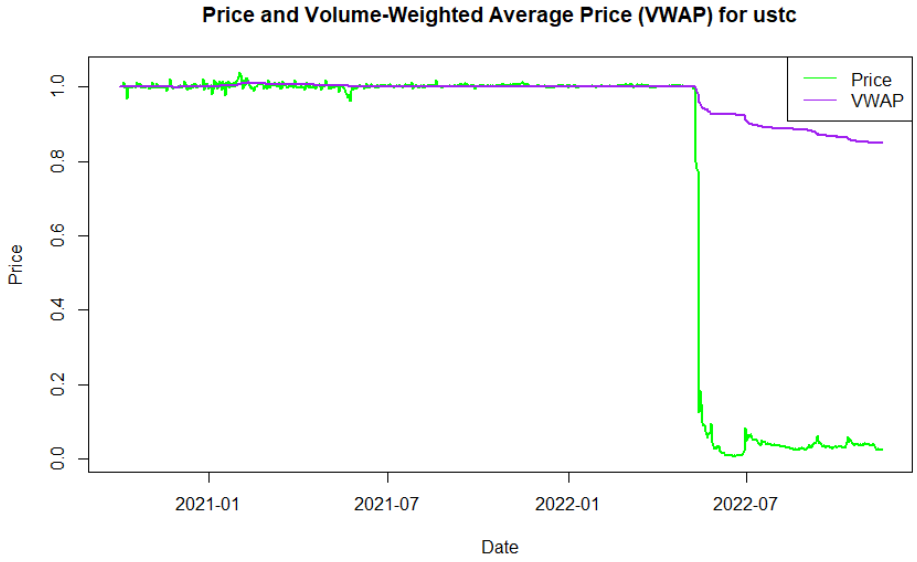

Figure 10. VWAP of USTC.

The divergence between price and VWAP illustrates the breakdown in price discovery mechanisms during the crisis. VWAP highlights how large trading volumes exacerbated price distortions, reflecting the market's inability to stabilize.

3.3. Prediction

In Table 3 the RNN predictions are perfect following the evolution of the USTC price trend, with a considerable increase from January 2021 to completely cancel out with the depeg event of the Luna crash in May of the same year. We evaluate, in this table, the predictive performance metrics of both recurrent neural networks (RNNs) with the H_2O package and k-NN with the Caret package for USTC price movements. Here, the RNN displays a mean squared error (MSE) of 0.2515, a root mean squared error (RMSE) of 0.5015, and log values indicative of effective trend tracking from early 2021 to the significant depeg event in 2022. The k-NN model shows slightly lower error rates (MSE: 0.1447, RMSE: 0.3804), suggesting its robustness in price prediction for the period. However, both models adeptly capture trend changes, with k-NN showing particular accuracy by historical pattern recognition in crypto markets like USTC.

Table 3. RNN and k-NN forecast statistics for USTC

USTC	MSE	RMSE	Mean Per-Class Error	Log-Loss
RNN	0.2515	0.5015		
k-NN	0.1447	0.3804	577.0863	

4. STAR Multivariate Analysis of LUNA Classic with Volumes as Exogenous Variables and USTC as Transition Variable

4.1. Database

As shown in Table 4, the database is composed of the previous variables, LUNC and USTC closing prices in daily frequency, accompanied by their volumes exchanged. To these series, we also add the volume of BTC as suggested by [1]. The period goes from 2 October 2020 to 15 November 2022.

Table 4. Database of the ST-VAR.

Variable	Mean	Median	Minimum	Maximum
LUNC	24.373	6.7102	4.67×10^{-6}	116.46
VOL_LUNC	8.98×10^{8}	4.38×10^{8}	1.06×10^{6}	1.65×10^{10}
USTC	0.76905	1.0009	0.006502	1.0392
VOL_USTC	1.82×10^{8}	6.87×10^{7}	16.194	5.98×10^{9}
VOL_BTC	3.85×10^{10}	3.19×10^{10}	1.17×10^{10}	4.29×10^{11}
Variable	**St. Dev.**	**C.V.**	**Skewness**	**Kurtosis**
LUNC	31.373	1.2872	1.1626	0.046461
VOL_LUNC	1.25×10^{9}	1.3955	4.3674	38.441
USTC	0.41261	0.53652	−1.2101	−0.52588
VOL_USTC	3.86×10^{8}	2.1198	7.726	88.937
VOL_BTC	3.02×10^{10}	0.78367	7.468	80.833
Variable	**PC 5%**	**PC 95%**	**IQ**	**Missing**
LUNC	9.70×10^{-5}	90.581	42.69	0
VOL_LUNC	4.53×10^{6}	2.93×10^{9}	1.23×10^{9}	0
USTC	0.025549	1.0094	0.033036	0
VOL_USTC	67132	7.57×10^{8}	1.44×10^{8}	0
VOL_BTC	1.61×10^{10}	7.20×10^{10}	2.10×10^{10}	0

Note: *LUNC* is the raw time series of the LUNA stablecoin. *VOL_LUNC* is the time series of volumes exchanged for LUNA. *USTC* is the raw time series of the USTC stablecoin. *VOL_USTC* is the time series of volumes exchanged for USTC. and *VOL_BTC* is the time series of volumes exchanged for Bitcoin. *St.Dev.* is the standard deviation. *PC*5% and *PC*95% are, respectively, the 5% and 95% percentiles. *IQ* is the interquartile amplitude, and *Missing* is the number of missing values.

4.2. VLSTAR Model

The multivariate smooth transition model is an extension of the smooth transition regression model introduced by [27] (see also [28]). We chose it for its ability to capture nonlinear relationships between variables (like trading volumes) and price movements, which are essential in market crashes. The general model is

$$y_t = \mu_0 + \sum_{j=1}^{p} \Phi_{0,j} y_{t-j} + A_0 x_t \cdot G_t(s_t; \gamma, c) \left[\mu_1 + \sum_{j=1}^{p} \Phi_{1,j} y_{t-j} + A_1 x_t \right] + \varepsilon_t$$

where μ_0 and μ_1 are the $\tilde{n} \times 1$ vectors of intercepts, $\Phi_{0,j}$ and $\Phi_{1,j}$ are square $\tilde{n} \times \tilde{n}$ matrices of the parameters for lags $j = 1, 2, \ldots, p$, A_0 and A_1 are $\tilde{n} \times k$ matrices of the parameters, x_t is the $k \times 1$ vector of exogenous variables and ε_t is the innovation. Finally, $G_t(s_t; \gamma, c)$ is an $\tilde{n} \times \tilde{n}$ diagonal matrix of the transition function at time t, such that

$$G_t(s_t; \gamma, c) = \{G_{1,t}(s_{1,t}; \gamma_1, c_1), G_{2,t}(s_{2,t}; \gamma_2, c_2), \ldots, G_{\tilde{n},t}(s_{\tilde{n},t}; \gamma_{\tilde{n}}, c_{\tilde{n}})\}$$

Each diagonal element $G^r_{i,t}$ is specified as a logistic cumulative density functions, i.e.,

$$G^r_{i,t}(s^r_{i,t}; \gamma^r_i, c^r_i) = \left[1 + \exp\left\{-\gamma^r_i \left(s^r_{i,t} - c^r_i\right)\right\}\right]^{-1}$$

for latex and $r = 0, 1, \ldots, m-1$, so that the first model is a Vector Logistic Smooth Transition AutoRegressive (VLSTAR) model. The ML estimator of θ is obtained by solving the optimization problem

$$\hat{\theta}_{ML} = \arg\max_{\theta} \log L(\theta)$$

where $\log L(\theta)$ is the log-likelihood function of the VLSTAR model, given by

$$ll(y_t \mid I_t; \theta) = -\frac{T\tilde{n}}{2} \ln(2\pi) - \frac{T}{2} \ln|\Omega| - \frac{1}{2} \sum_{t=1}^{T} \left(y_t - \tilde{G}_t B z_t\right)' \Omega^{-1} \left(y_t - \tilde{G}_t B z_t\right)$$

The NLS estimators of the VLSTAR model are obtained by solving the optimization problem

$$\hat{\theta}_{NLS} = \arg\min_{\theta} \sum_{t=1}^{T} \left(y_t - \Psi'_t B' x_t\right)' \left(y_t - \Psi'_t B' x_t\right).$$

Generally, the optimization algorithm may converge to some local minimum. For this reason, providing valid starting values of θ is crucial. If there is no clear indication on the initial set of parameters, θ, this can be carried out by implementing a grid search. Thus, a discrete grid in the parameter space of Γ and C is created to obtain the estimates of B conditionally on each point in the grid. The initial pair of Γ and C producing the smallest sum of squared residuals is chosen as the initial values, and then the model is linear in parameters. The algorithm is the following:

1. A construction of the grid for Γ and C, computing Ψ for each point in the grid;
2. An estimation of $\hat{B}$ in each equation, calculating the residual sum of squares, Q_t;
3. Finding the pair of Γ and C providing the smallest Q_t;
4. Once the starting values have been obtained, an estimation of parameters, B, via nonlinear least squares (NLS);
5. An estimation of Γ and C, given the parameters found in step 4;
6. Repeat steps 4 and 5 until convergence.

4.3. Model Estimation

We specify the model estimated with our variables.

$$\begin{pmatrix} y_{l,t} \\ y_{u,t} \end{pmatrix} = \varphi \begin{pmatrix} y_{l,t-1} \\ y_{u,t-1} \end{pmatrix} + A \begin{pmatrix} x_{vl,t} \\ x_{vu,t} \\ x_{vb,t} \end{pmatrix} \equiv \begin{pmatrix} r \text{ lunc }_t \\ r \text{ ustc }_t \end{pmatrix} = \varphi \begin{pmatrix} r \text{ lunc } c_{t-1} \\ r \text{ ustc } c_{t-1} \end{pmatrix} + A \begin{pmatrix} r \text{ vol.lunc }_t \\ r \text{ vol.ustc }_t \\ r \text{ vol. btc }_t \end{pmatrix} \quad (1)$$

$$\begin{aligned} y_{l,t} &= \text{ rlunc }_t = \text{ returns LUNC;} \\ y_{u,t} &= \text{ rustc }_t = \text{ returns USTC;} \\ y_{l,t-1} &= \text{rlunc}_{t-1} = \text{ lagged returns of LUNC;} \\ y_{u,t-1} &= \text{ rustc }_{t-1} = \text{ lagged returns of l'USTC;} \\ x_{vl,t} &= \text{ rvol. lunc }_t = \text{ returns of LUNC volumes;} \\ x_{vu,l} &= \text{ rvol. } ustc_t = \text{ returns of USTC volumes;} \\ x_{vb,t} &= \text{ rvol. } btc_t = \text{ returns of Bitcoin volumes.} \end{aligned} \quad (2)$$

After experimenting, s_t is set as the squared log-differenced LUNC series. Regarding the starting values of the Gamma and C parameters, we proceed to a grid-search by setting the number of combinations for the searching grid to 3, and the number of iterations is equal to 500.

The ST-VAR model was applied to a comprehensive dataset comprising volatility series from our three variables over October 2020 to November 2022 to analyze the interdependencies and dynamics between these factors. The ST-VAR model results provide valuable insights into the relationships and behaviors of the volatilities under investigation. The following observations and interpretations can be drawn from the analysis:

In Table 5, we highlight several important findings. The LUNA price crash in regime two reports higher coefficients than in regime one (at 1% statistical error). This finding applies to the volumes of LUNA as well. This confirms that the firesale of LUNA with heavy volumes dramatically impacted its price path during regime two.

Table 5. VLSTAR model estimate of LUNC-USTC pair with volumes as exogenous variables.

Model VLSTAR with 2 regimes Full sample size: 773 Number of estimated parameters: 32 Multivariate log-likelihood: 6097.746					
Equation y1					
Coefficient regime one					
const	lunc.r	ustc.r	vol.lunc.r	vol.USTC.r	vol.btc.r
0.443	0.003	0.005	0.071 ***	−0.005	−0.040
Coefficient regime two					
const	lunc.r	ustc.r	vol.lunc.r	vol.USTC.r	vol.btc.r
−83.791 ***	0.391 ***	−0.759 ***	1.040 ***	-0.467 ***	0.078 **
Gamma: 1.3112	c: 1002.592				
AIC: 5470.98	BIC: 5526.79	LL: −2723.49			
Equation y2					
Coefficient regime one					
const	lunc.r	ustc.r	vol.lunc.r	vol.USTC.r	vol.btc.r
−0.411	0.072 ***	−0.112 ***	0.022 ***	0.002	−0.009
Coefficient regime two					
const	lunc.r	ustc.r	vol.lunc.r	vol.USTC.r	vol.btc.r
−6.371 ***	0.121 ***	−0.176 ***	0.063 ***	0.105 ***	−0.007
Gamma: 42.92	c: 189.629				
AIC: 3960.34	BIC: 4016.14	LL: −1968.17			

Note: *const* stands for the constant term, *lunc.r* for LUNA log-returns, *ustc.r* for USTC log-returns, *vol.lunc.r* for the volumes exchanged of LUNA, *vol.USTC.r* for the volumes exchanged of USTC, and *vol.btc.r* for the volumes exchanged of Bitcoin. *LL* stands for log-likelihood. ***: statistically highly significant ($p < 0.01$); **: statistically significant ($p < 0.05$).

Interestingly, the volumes of USTC are also significant at the 1% level during regime two. The stablecoin drops and the pyramid falls.

It is noteworthy to remark that, similarly to [1], we uncover the statistically significant effect of Bitcoin volumes on the LUNA price crash during regime two.

The significance tests conducted on the coefficient estimates indicate that the majority of the coefficients are statistically significant at the 1% level, providing confidence in the estimated relationships between the variables. However, some coefficients did not reach statistical significance, implying a need for a cautious interpretation of these specific relationships.

The ST-VAR model assumes stationarity, exogeneity, and the absence of serial correlations among the residuals [17]. While the stationarity assumption appears reasonable based on preliminary tests, further analysis is required to confirm the exogeneity assumption and explore any potential serial correlation in the residuals (see Section 4.4).

In conclusion, the ST-VAR model results provide valuable insights into the interdependencies and dynamics between the variables under investigation. The positive and significant coefficients for BTC and the inverse relationship observed for USTC highlight the importance of these variables in the system. These important findings have implications for investors, crypto market's professionals and researchers who seek to understand the impacts of these variables on the fall of the Terra platform. However, it is important to acknowledge the limitations and assumptions of the model and consider further analysis to validate and refine the conclusions with more datasets and potential extensions to account for other relevant factors.

We describe the graph output from the VLSTAR model with two endogenous variables (LUNC and USTC) and three exogenous variables (the volumes of LUNC, USTC and Bitcoin). All variables have been transformed into stationarity by taking first the log differences.

Figure 11 illustrates the daily percentage returns of LUNC. We witness the explosive nature of the LUNC asset toward May 2022, as reproduced by the VLSTAR model. This pronounced volatility, particularly during the crash, highlights the asset's sensitivity to market events. Short-term spikes reflect speculative trading and potential market inefficiencies, while the drastic drop during the crash emphasizes systemic risk. This underscores the importance of analyzing how algorithmic failures, coupled with external factors, amplify volatility in cryptocurrency markets.

Figure 12 of USTC returns showcases a dramatic shift in market dynamics around the depeg with the US dollar period (May 2022), as reproduced by the VLSTAR model. The high-frequency oscillations during and after the depeg event signify heightened uncertainty and speculative behavior. This figure supports the narrative that stablecoin instability can destabilize interconnected assets, demonstrating the fragility of algorithmic models underpinning such systems.

In Figure 13, the volume analysis for LUNC provides a measure of market activity and liquidity over time, as reproduced by the VLSTAR model. The heightened volume of exchange for the LUNA asset during the crash signifies panic selling and herd behavior, aligning with periods of maximum uncertainty. Such trends indicate that market participants respond disproportionately to negative shocks, leading to feedback loops that exacerbate price declines.

In Figure 14, we find that similar to LUNC, the trading volume for USTC reflects significant spikes during critical periods of instability, as reproduced by the VLSTAR model. This pattern underscores the role of USTC as a central piece in the Terra ecosystem, where its instability directly affected investor sentiment and trading behavior, leading to cascading effects on LUNC.

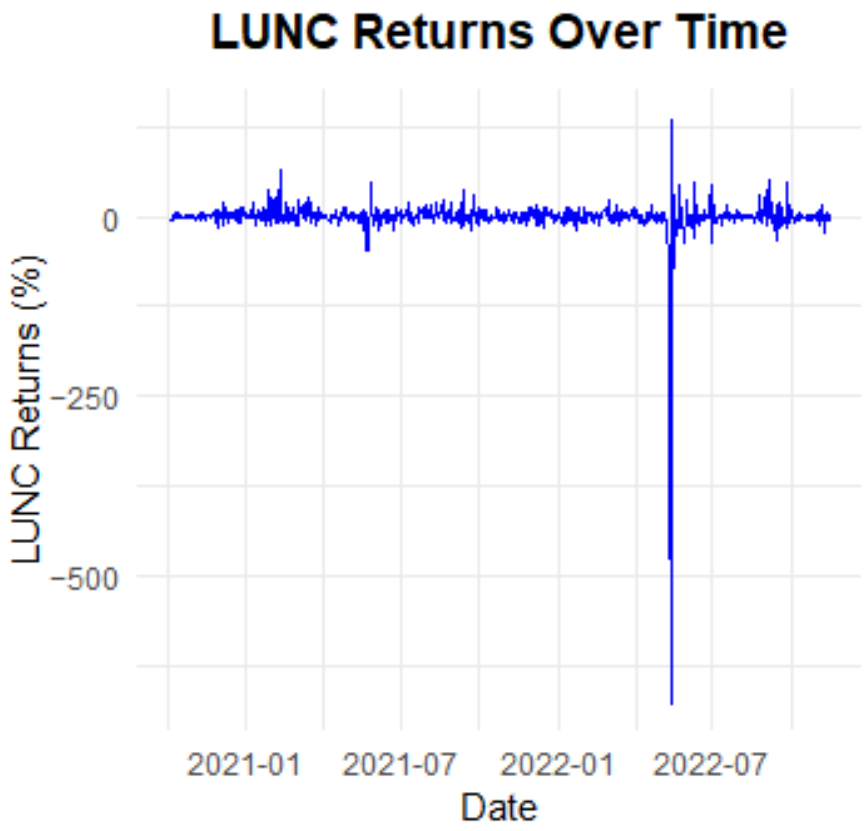

Figure 11. VLSTAR estimate of endogenous LUNA Classic.

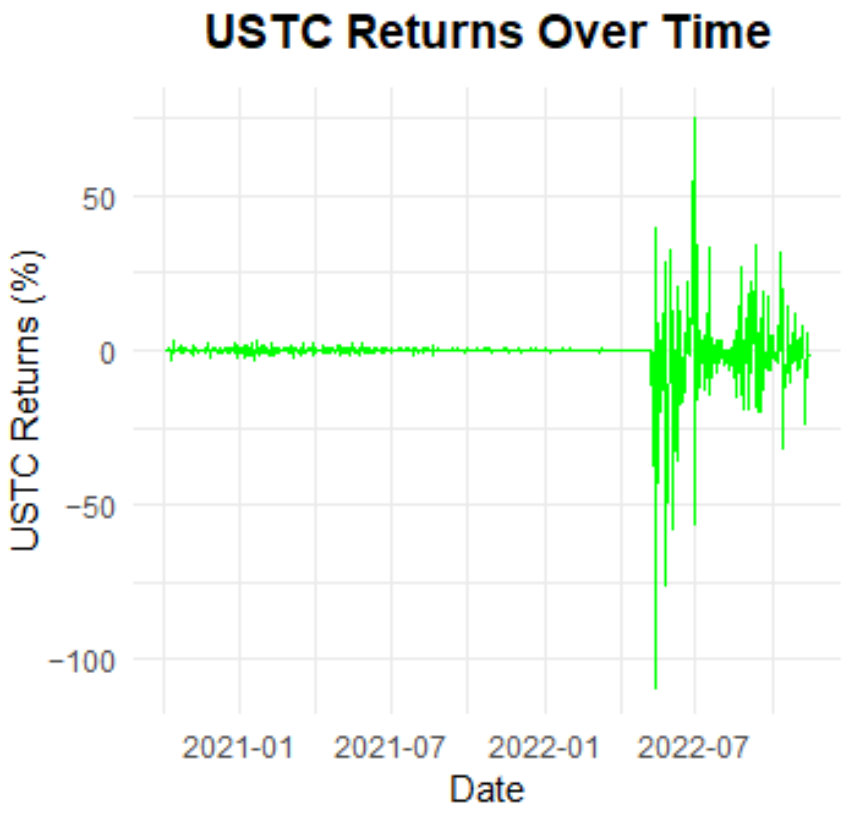

Figure 12. VLSTAR estimate of endogenous USTC stablecoin.

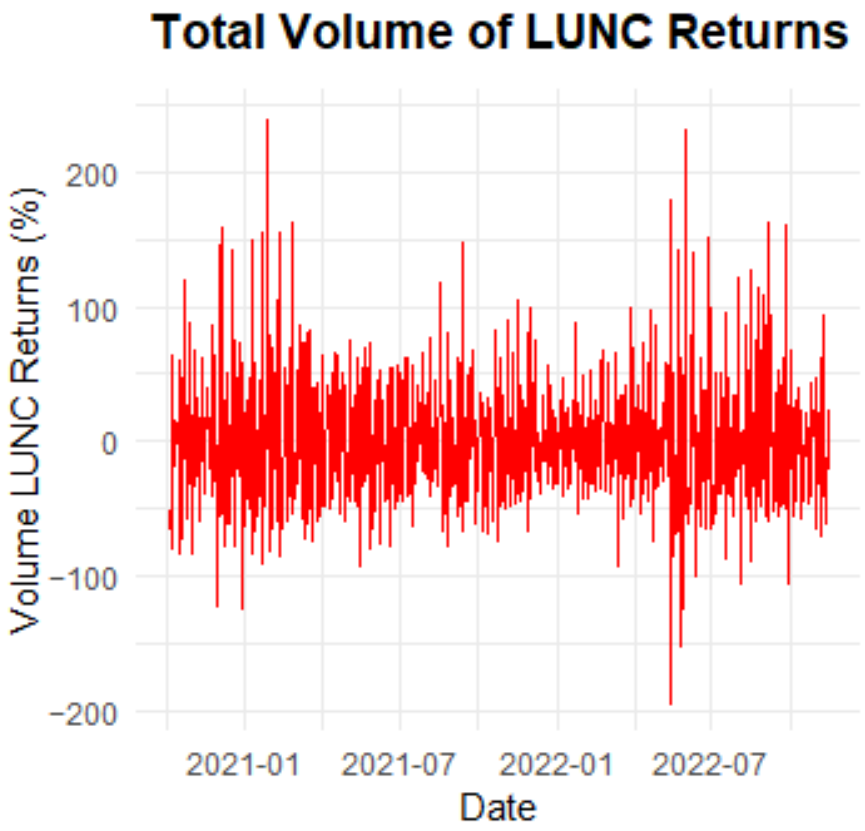

Figure 13. VLSTAR estimate of exogenous impact of LUNA volumes on LUNC.

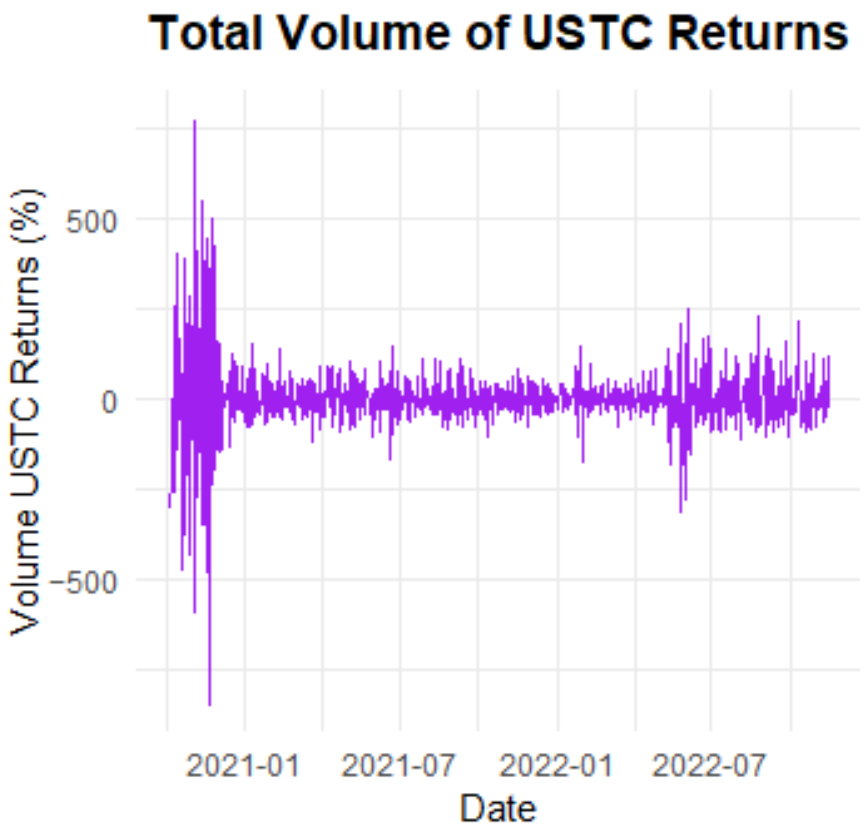

Figure 14. VLSTAR estimate of exogenous impact of USTC volumes on LUNC.

In Figure 15, we can confirm the hypothesis by [1] that the volumes of Bitcoin (especially short positions) have also played a role during the first phase of the underlying disengagement of LUNA Classic, as reproduced by the VLSTAR model. We know that the LUNA Foundation established a BTC reserve with the intention of burning it to help stabilize the USTC's depeg. Indeed, including BTC as a benchmark allows for a comparative understanding of systemic spillover effects. The relatively subdued volume spikes in BTC suggest that while the crash of USTC and LUNC was significant within the Terra ecosystem, its broader impact on the crypto market was limited. This aligns with BTC's position as a relatively stable and mature asset in the cryptocurrency hierarchy.

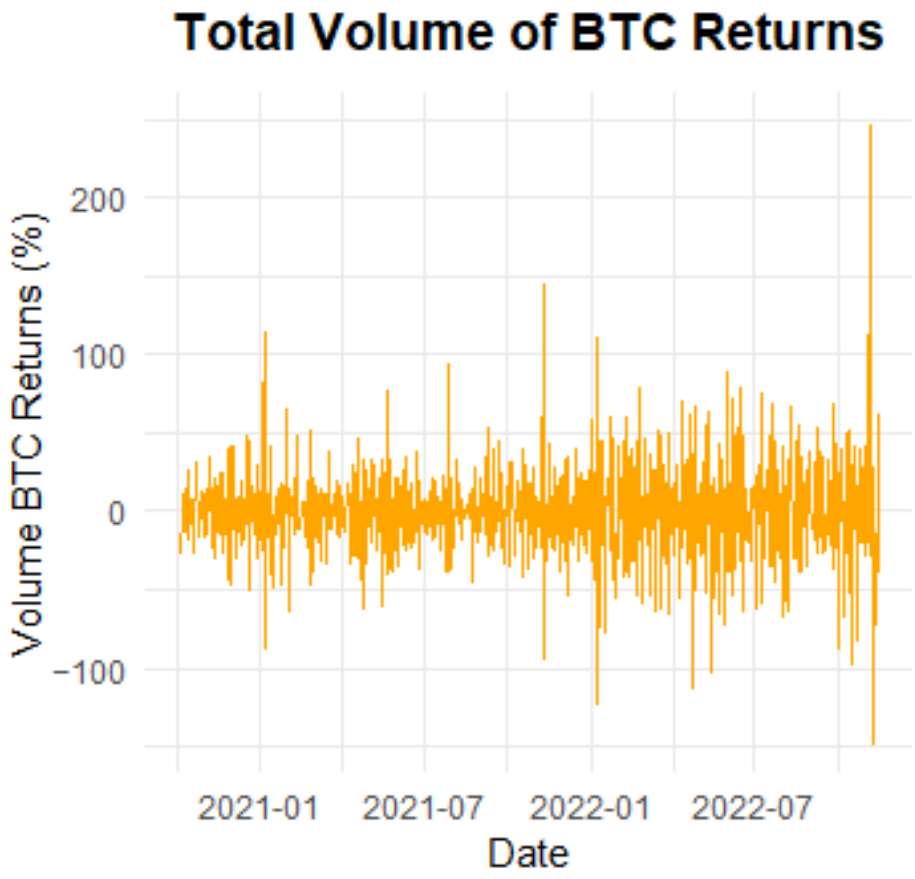

Figure 15. VLSTAR estimate of exogenous impact of Bitcoin volumes on LUNC.

The application of the STAR (Smooth Transition AutoRegressive) model to the LUNA price crash reveals important nonlinear dynamics between trading volumes and price movements during different market regimes, particularly in the aftermath of the USTC depeg. The model's regime-switching mechanism highlights the fact that the market behaved differently in the two distinct phases: pre depeg and post depeg. During regime two (post depeg), the model identifies significantly higher coefficients, particularly in relation to trading volumes, indicating that the massive volume of trades—driven by investor panic and fire sales—had a much more pronounced and nonlinear impact on LUNA's price decline than in the earlier regime. This shift underscores the critical role of liquidity in cryptocurrency markets, where a sudden loss of confidence can trigger cascading price collapses, magnified by large-scale liquidations. We can highlight some practical implications:

1. Liquidity Crises in Crypto Markets: The findings offer valuable insights into how liquidity crises unfold in highly volatile and speculative markets like cryptocurrency. Specifically, they show that the interaction between trading volumes and price dynam-

ics is not linear; rather, once certain thresholds are crossed—such as the USTC losing its peg—the market enters a regime where liquidity evaporates, leading to extreme price fluctuations. This is particularly relevant for investors and market participants, as it highlights the fragile nature of liquidity in these markets and the potential for a price collapse to be triggered or exacerbated by large trading volumes.

2. Risk Management for Stablecoin Ecosystems: For stablecoin ecosystems, which rely on the algorithmic maintenance of pegs (such as the Terra-LUNA system), the nonlinear impact of trading volumes revealed by the model points to the need for robust risk management mechanisms that can prevent or mitigate large-scale liquidations. The Terra-LUNA crash demonstrates that when liquidity is constrained, even small disruptions can lead to disproportionate effects on the price, underscoring the importance of designing stablecoin systems that can absorb shocks more effectively.
3. Implications for Algorithmic Stablecoins: The findings also have broader implications for the design and regulation of algorithmic stablecoins. The collapse of LUNA highlights the vulnerability of stablecoins that rely on algorithmic adjustments and collateral reserves, particularly in volatile markets. The sharp transition between regimes in the STAR model suggests that algorithmic stablecoins are prone to instability under certain market conditions, calling for improved design features that can better manage liquidity and maintain peg stability in times of market stress.
4. Policy and Regulatory Considerations: From a policy perspective, the insights drawn from the STAR model's estimation results could inform regulatory frameworks for stablecoins and other digital assets. Regulators may consider imposing safeguards that ensure better liquidity management and transparency in collateral reserves, reducing the risk of market crashes driven by large-scale liquidations. This is particularly pertinent in light of the systemic risks that such crashes pose to the broader cryptocurrency market.
5. Future Risk Models: For researchers and practitioners, the model's findings suggest that future risk models for stablecoins and other digital assets should account for nonlinearities in trading volume and price dynamics. The STAR model's ability to capture these nonlinear shifts provides a more accurate tool for understanding and predicting the conditions under which digital assets might experience extreme price volatility and should be integrated into the risk models used by market participants, exchanges, and financial institutions dealing with cryptocurrencies.

By demonstrating the transition between different market regimes and the heightened sensitivity to trading volumes during the post-depeg phase, the STAR model offers a valuable framework for analyzing and predicting the behavior of digital assets in crisis situations. This can ultimately contribute to the development of more resilient stablecoin ecosystems and risk mitigation strategies in cryptocurrency markets.

4.4. Robustness Checks

4.4.1. A Linearity Test

As a robustness check, we implement a joint linearity test. Given a VLSTAR model with a unique transition variable, $s_{1t} = s_{2t} = \ldots = s_{nt} = s_t$, a generalization of the linearity test presented in [29,30] may be implemented. We assume a two-state VLSTAR model, such that

$$y_t = B_1 z_t + G_t B_2 z_t + \varepsilon_t$$

where the null $H_0 : \gamma_j = 0, j = 1, \ldots, \tilde{n}$, is such that $G_t \equiv (1/2)/\tilde{n}$ and the previous equation is linear. When the null cannot be rejected, an identification problem of the parameter c_j in the transition function emerges, which can be solved through a first-order Taylor expansion around $\gamma_j = 0$. The approximation of the logistic function with a first-order Taylor expansion is given by

$$G(s_t;\gamma_j,c_j) = (1/2) + (1/4)\gamma_j(s_t - c_j) + r_{jt}$$
$$= a_j s_t + b_j + r_{jt}$$

where $a_j = \gamma_j/4, b_j = 1/2 - a_j c_j$ and r_j is the error of the approximation. If G_t is specified as follows

$$G_t = \text{diag}\{a_1 s_t + b_1 + r_{1t}, \ldots, a_{\tilde{n}} s_t + b_{\tilde{n}} + r_{\tilde{n}t}\}$$
$$= As_t + B + R_t$$

where $A = \text{diag}(a_1, \ldots, a_{\tilde{n}}), B = \text{diag}(b_1, \ldots, b_{\tilde{n}})$ e $R_t = \text{diag}(r_{1t}, \ldots, r_{\tilde{n}t}), y_t$ can be written as

$$y_t = B_1 z_t + (As_t + B + R_t)B_2 z_t + \varepsilon_t$$
$$= (B_1 + BB_2)z_t + AB_2 z_t s_t + R_t B_2 z_t + \varepsilon_t$$
$$= \Theta_0 z_t + \Theta_1 z_t s_t + \varepsilon_t^*$$

where $\Theta_0 = B_1 + B_2' B, \Theta_1 = B_2' A$ and $\varepsilon_t^* = R_t B_2 + \varepsilon_t$. Under the null, $\Theta_0 = B_1$ and $\Theta_1 = 0$, while the previous model is linear, with $\varepsilon_t^* = \varepsilon_t$. It follows that the Lagrange multiplier test, under the null, is derived from the score

$$\frac{\partial \log L(\widetilde{\theta})}{\partial \Theta_1} = \sum_{t=1}^{T} z_t s_t \left(y_t - \widetilde{B}_1 z_t\right)' \widetilde{\Omega}^{-1} = S\left(Y - Z\widetilde{B}_1\right)\widetilde{\Omega}^{-1}$$

where

$$S = z_1' s_1 \vdots z_t' s_t$$

and where $\widetilde{B}_1$ and $\widetilde{\Omega}$ are estimated from the model in H_0. If $P_Z = Z(Z'Z)^{-1}Z'$ is the projection matrix of Z, the LM test is specified as follows

$$LM = \text{tr}\left\{\widetilde{\Omega}^{-1}\left(Y - Z\widetilde{B}_1\right)' S\left[S'(I_t - P_Z)S\right]^{-1} S'\left(Y - Z\widetilde{B}_1\right)\right\}$$

Under the null, the test statistics is distributed as χ^2 with $\tilde{n}(p \cdot \tilde{n} + k)$ degrees of freedom.

Table 6 contains the results of the procedure detailed above regarding the adequacy of the VLSTAR model.

To test the robustness of the results, alternative lag orders and variable combinations were examined by a joint linearity test [17]. The main conclusions drawn from the ST-VAR model remained consistent across these variations, indicating the reliability of the findings. Table 6 reveals that the VLSTAR specification is the most accurate model to model jointly the nonlinearities at stake between the variation in the LUNC and USTC, on the one hand, and the volumes associated with LUNC, USTC and BTC on the other hand.

Table 6. Joint linearity test.

	Joint Linearity Test	**Decision**
p-value	0.0001	VLSTAR
Diagnostics		
LM	839	
Critical value for alpha	23.3	

4.4.2. GARCH Model with Dummy

The model used is a standard GARCH(1,1) model with one external regressor (the crash dummy variable) to capture the impact of the Terra-LUNA crash event. GARCH with the dummy model provides a clear view of volatility clustering and persistence during the LUNA crash, capturing how volatility was strongly influenced by recent shocks (alpha1) and remained elevated over time (beta1). The model shows that volatility during the crash period was driven primarily by endogenous market responses rather than by isolated shocks, evidenced by the insignificance of the dummy variable. However, while

GARCH with the dummy model captures general volatility clustering and persistence in the LUNA price series during the USTC depeg, diagnostic tests (e.g., residual autocorrelation, goodness of fit) suggest it may miss certain finer points, like the asymmetric impact of negative news, typical during crises. Indeed, it does not consider asymmetric effects (i.e., different impacts of positive vs. negative shocks). The Table 7 shows the summary of the GARCH with dummy models results.

The log-likelihood (−2824.132) is an important fit measure, though it is slightly lower compared to more complex models (e.g., TGARCH). This suggests that the model captures general volatility patterns but may not fully account for asymmetrical responses in volatility during crashes.

The information criteria Akaike (AIC = 7.3078) and Bayesian (BIC = 7.3319) values provide a basis for comparing model performance; here, they indicate a reasonable fit, but further refinement might be achieved by exploring asymmetry in volatility (e.g., TGARCH).

Omega (ω = 5.3875, p = 0.0078) represents the baseline volatility level, which is significant and elevated, reflecting a generally high-volatility environment around the time of the crash. This aligns with the heightened uncertainty and rapid price swings seen in LUNA's market as USTC's peg failed.

Alpha ($\alpha 1$ = 0.6619, $p < 0.001$) shows that recent shocks have a strong, immediate impact on volatility. This means that each new price drop or sudden trading volume increase directly spikes volatility, which is typical during crisis periods with cascading panic sell-offs.

Beta ($\beta 1$ = 0.5410, $p < 0.001$) reflects the persistence of high volatility, indicating that once volatility rises, it remains elevated for an extended period. In the context of the LUNA crash, this implies prolonged market instability following the initial depeg event, as investors continued to react to an uncertain environment.

The dummy variable's (vxreg1 = 0.0000, p = 1.0000) insignificance implies that the market volatility following the depeg event may have been driven endogenously rather than by a single discrete external shock. This suggests a feedback loop where market responses to price changes continuously spurred volatility, rather than volatility being tied directly to the USTC depeg event.

In brief, GARCH with the dummy model provides valuable insights into the general volatility dynamics of the LUNA crash. It confirms that volatility was high and persistent, reflecting the ongoing instability that followed the USTC depeg. However, the model's limitations lie in its assumption of symmetric volatility responses and the insignificance of the dummy variable, suggesting that the crisis-driven volatility was driven by market-endogenous dynamics rather than isolated external shocks. For a deeper and detailed study of the LUNA crash, these findings could be supplemented by an asymmetric model like TGARCH to capture the larger impact of negative shocks, providing a more comprehensive view of how volatility was affected during the crisis.

Table 7. Summary of GARCH with dummy model results.

Parameter/Statistic	Estimate	Std. Error	t-Value	*p*-Value	Interpretation
Omega (ω)	5.3875	2.0262	2.6589	0.0078	Baseline volatility, significant and elevated, indicating a high-volatility environment around the crash.
Alpha1 (α_1)	0.6619	0.0796	8.3131	$<$0.001	Short-term impact of shocks on volatility; high alpha indicates strong immediate volatility response.
Beta1 (β_1)	0.5410	0.0358	15.1133	$<$0.001	Volatility persistence; significant beta suggests volatility remains high for extended periods post shock.
Dummy Variable (vxreg1)	0.0000	2.0076	0.0000	1.0000	Insignificant, suggesting that volatility was endogenously driven rather than by a single shock event.
Log-Likelihood	$-$2824.132	-	-	-	Indicates model fit, with further improvement possible via models capturing asymmetry (e.g., TGARCH).
Akaike Information Criterion (AIC)	7.3078	-	-	-	Basis for model comparison; reflects reasonable fit but highlights room for enhancement.
Bayesian Information Criterion (BIC)	7.3319	-	-	-	Provides basis for model selection, showing potential for exploring alternative models.
Weighted Ljung–Box (Residuals)	-	-	-	p = 0.04463 (Lag 5)	Mixed results at certain lags, suggesting model may miss finer patterns in residual autocorrelation.
ARCH LM Test	-	-	-	$p > 0.5$	No additional ARCH effects detected, indicating GARCH(1,1) specification captures clustering well.
Nyblom Stability Test (Joint)	1.5409	-	-	-	Confirms parameter stability, indicating consistent volatility dynamics across the sample period.
Sign Bias Test (Joint Effect)	3.3332	-	-	0.3431	No significant bias detected; supports use of symmetric model, though TGARCH may capture asymmetry better.
Adjusted Pearson Goodness of Fit	102.7 (group 1)	-	-	$p < 0.001$	Significant p-values suggest model fit limitations, warranting further exploration of volatility dynamics.

4.4.3. TGARCH Model with Dummy

The TGARCH model (fGARCH sub-model: TGARCH(1,1)) is designed to capture volatility asymmetry, specifically highlighting the differential impact of positive and negative shocks on market volatility. The model TGARCH (Threshold GARCH) with the dummy provides a nuanced understanding of the volatility dynamics during the LUNA crash by accounting for asymmetric responses to positive and negative shocks. This feature makes it particularly suitable for analyzing the market behavior around the USTC depeg and LUNA's subsequent price collapse. The Table 8 shows the summary of the TGARCH with dummy models results.

The log-likelihood (−2806.026) is higher than the log-likelihood of the simpler GARCH model. This improvement suggests that the TGARCH model captures more nuances in the data, particularly asymmetries, making it better suited for crises like the Terra-LUNA crash.

The Akaike (AIC = 7.2636) and Bayesian (BIC = 7.2937) values are slightly lower than the GARCH model, reinforcing that TGARCH provides a better fit by capturing volatility asymmetry.

The parameter of baseline volatility omega ($\omega = 0.78044$, $p = 0.000166$) is statistically significant. The lower value compared to GARCH's omega suggests that TGARCH provides a more precise baseline, adjusting for volatility spikes due to asymmetrical shock responses.

Alpha1 ($\alpha 1 = 0.45656$, $p < 0.001$) shows that recent shocks significantly influence current volatility. A moderately high alpha indicates that LUNA's market volatility was immediately impacted by each recent shock, with fast adjustments in response to new information or sell-offs.

Beta1 ($\beta 1 = 0.62674$, $p < 0.001$) represents the persistence of volatility over time, meaning high volatility remains elevated after shocks. This persistence aligns with the prolonged instability during the Terra-LUNA crash period, where volatility lingered as investors struggled to regain confidence.

Eta11 (Eta11 = 0.18420, $p = 0.00126$) captures the asymmetry in volatility responses, where negative shocks (e.g., price drops) lead to larger volatility spikes than positive shocks. This significant eta value indicates that volatility increased disproportionately when prices fell, capturing the heightened panic during the USTC depeg. This is a key finding as it confirms that market responses to negative news were stronger and contributed to the self-reinforcing crash dynamics.

The insignificance of the dummy variable (vxreg1 = 0.00000, $p = 1.0000$) implies that the crash's impact on volatility was primarily endogenous. Market volatility seemed to respond more to internal feedback loops rather than an isolated external shock, consistent with a cascading market reaction post depeg.

We also highlight some of the other most relevant pieces of information and statistical metrics in the table.

The TGARCH model's ability to account for asymmetric volatility—where negative shocks increase volatility more than positive ones—aligns with the market behavior observed during the LUNA crash. Negative news (USTC depeg) disproportionately escalated volatility, a pattern typical of financial crises, making TGARCH with the dummy a more appropriate model for this analysis compared to GARCH with the dummy. This model underscores the systemic risks of endogenous feedback loops in unregulated crypto assets and provides a critical perspective for policymakers on the dangers of algorithmic stablecoin designs.

Table 8. Summary of TGARCH with dummy model results.

Parameter/Statistic	Estimate	Std. Error	t-Value	*p*-Value	Interpretation
Omega (ω)	0.7804	0.2072	3.7657	0.000166	Baseline volatility, significant and elevated, reflecting a high-volatility environment during the crash.
Alpha1 (α_1)	0.4566	0.0386	11.8377	$<$0.001	Short-term shock impact; high alpha indicates strong immediate volatility response to recent shocks.
Beta1 (β_1)	0.6267	0.0317	19.7426	$<$0.001	Persistence of volatility; high beta suggests volatility remains high after shocks, aligning with prolonged instability.
Eta11 (η_{11})	0.1842	0.0571	3.2248	0.00126	Asymmetry term; significant eta confirms larger volatility responses to negative shocks, key for modeling crash dynamics.
Dummy Variable (vxreg1)	0.0000	0.1668	0.0000	1.0000	Insignificant, indicating endogenous volatility dynamics driven by market response rather than a single shock event.
Log-Likelihood	-2806.026	-	-	-	Indicates model fit, with higher log-likelihood than GARCH model, showing TGARCH captures volatility asymmetry better.
Akaike Information Criterion (AIC)	7.2636	-	-	-	Basis for model comparison, showing improved fit over GARCH and confirming TGARCH's appropriateness for asymmetry.
Bayesian Information Criterion (BIC)	7.2937	-	-	-	Reflects model fit and suitability for capturing volatility asymmetry in the Terra-LUNA crash.
Weighted Ljung–Box (Residuals)	-	-	-	$p = 0.024319$ (Lag 2)	Some residual autocorrelation suggests minor fit limitations at certain lags, though model performs well overall.
ARCH LM Test	-	-	-	$p > 0.5$	No additional ARCH effects, indicating that the TGARCH model captures volatility clustering adequately.
Nyblom Stability Test (Joint)	1.4135	-	-	-	Confirms parameter stability, indicating consistent volatility dynamics across the sample period.
Sign Bias Test (Negative Sign Bias)	1.7263	-	-	$p = 0.08469$	Mild evidence of negative sign bias, suggesting a greater response to negative shocks, in line with TGARCH design.
Adjusted Pearson Goodness of Fit	89.88 (group 1)	-	-	$p = 3.489 \times 10^{-11}$	Significant *p*-values indicate some fit limitations, supporting further exploration of market response dynamics.

4.4.4. Comparison Table Including GARCH with Dummy Model Alongside the TGARCH with Dummy and Linearity Test (STVAR)

The Table 9 is a comparison table including GARCH with the dummy model alongside TGARCH with the dummy and linearity test (STVAR):

We can mention how TGARCH better models volatility dynamics by accounting for asymmetry, while the STVAR model (supported by the linearity test) captures regime-dependent relationships, together providing a fuller understanding of the LUNA crash. The GARCH model assumes that both positive and negative shocks affect volatility in the same way. However, the LUNA crash was characterized by panic-driven negative shocks, where bad news (such as the USTC depeg) caused disproportionate volatility increases. This is where GARCH falls short, as it does not account for this asymmetry. The insignificance of the dummy variable implies that the USTC depeg event did not create a distinct break in volatility patterns. Instead, market dynamics, likely driven by endogenous reactions to price changes, were the main drivers of volatility.

Table 9. Comparison table of the three models.

Aspect	GARCH with Dummy	TGARCH with Dummy	Linearity Test (STVAR)
Focus	Basic volatility modeling without asymmetry	Volatility dynamics with asymmetry for positive vs. negative shocks	Detecting nonlinearity in relationships between variables (e.g., price and volumes)
Type of Model	Standard GARCH (with a dummy variable)	Threshold GARCH (TGARCH) with a dummy variable	Linearity test to validate the nonlinearity and regime-switching nature of STVAR
Key Feature	Symmetric volatility response to shocks	Asymmetric volatility response to shocks	Nonlinear transitions between market regimes (pre and post crash)
Volatility	Models volatility clustering and persistence	Models volatility clustering, persistence, and asymmetry	Not focused on volatility; more on dynamic relationships between variables
Shocks Handling	Models equal impact of positive and negative shocks	Negative shocks have larger impacts on volatility	Models shifts in relationships (e.g., price–volume) between regimes
Regime Shifts	Dummy variable attempts to capture regime shifts	Dummy variable attempts to capture regime shifts but is insignificant	Identifies regime changes through smooth transitions in variables
Relevance to Crash	Shows general volatility increase post depeg	Shows greater volatility response to negative shocks, capturing heightened sensitivity to crashes	Explains regime-dependent relationships, capturing how variables (e.g., price, volume) interact differently post crash
Event Modeling	Dummy variable included but lacks significance	Dummy variable included but insignificant	Implicitly models regime shifts using nonlinear transitions in STVAR

In summary, the TGARCH model complements the VLSTVAR model but does not replace it; they serve different purposes. Both TGARCH with the dummy and the VLSTAR model address different aspects of the LUNA crash. The TGARCH model focuses on volatility and the asymmetric impact of negative shocks, showing that the crash had a disproportionate effect on market instability. The VLSTVAR (validated by the linearity test) model focuses on how relationships between variables changed across different regimes (before and after the crash) and nonlinear dynamics during the crash. Both models contribute valuable insights into how the market reacted and transitioned during the USTC depeg event.

5. Conclusions

This paper investigates the collapse of LUNA Classic in the wake of the USTC depeg, using advanced econometric and time series methods such as the VLSTAR model. The results provide critical insights into the dynamics of algorithmic stablecoins and their susceptibility to liquidity crises, highlighting the role of large trading volumes and collateral assets like Bitcoin in amplifying the crash.

The collapse of USTC's peg demonstrated the fragility of algorithmic stablecoins, where the failure of the stabilization mechanism led to a cascading market crash. The inability to absorb the liquidity shock underlined systemic risks inherent in such systems. The role of collateral assets is well elucidated by our analysis. Bitcoin volumes were shown to have a significant effect on the LUNA price collapse, suggesting that the liquidity of collateral assets plays a pivotal role in maintaining price stability during crises. Our study also highlights the impact of trading volumes on price dynamics. Indeed, the analysis reveals that during regime two (post depeg), the large trading volumes significantly intensified the price crash. This nonlinear relationship underscores how liquidity shortages during large-scale liquidations can lead to dramatic price declines.

These interesting findings demonstrate how algorithmic stablecoin failures, like the USTC depeg, can amplify market instability, creating conditions where negative news drives disproportionately higher volatility. These findings also have implications for stakeholders:

- Investors: The findings highlight the vulnerabilities of algorithmic stablecoins, especially during periods of market stress. Investors should be aware of the potential for large-scale liquidations to rapidly destabilize prices, particularly in assets that rely on algorithmic mechanisms. This study emphasizes the need for better risk management strategies to mitigate such crashes.
- Researchers: For researchers, this study contributes to a deeper understanding of the nonlinear interactions between liquidity, volumes, and price movements in cryptocurrency markets. The VLSTAR model's ability to capture regime shifts offers a useful framework for analyzing other cryptocurrencies and volatile markets in the future.
- Policymakers: The results have regulatory implications, particularly for the design and oversight of stablecoins. Policymakers should consider imposing stricter safeguards to ensure liquidity and stability in algorithmic stablecoins, including requirements for transparent reserves and the ability to withstand large-scale liquidations.

However, while this study provides important insights, it also has several limitations:

1. Data Frequency: The analysis relies on daily frequency data, which may not fully capture intraday price volatility and rapid market reactions during the crash. Future research could utilize higher-frequency data to offer a more granular view of price dynamics.
2. Model Limitations: The VLSTAR model effectively captures nonlinear relationships, but alternative models such as GARCH could provide additional insights into volatility clustering and the behavior of prices during extreme events. Future studies could compare different modeling approaches to better understand the robustness of the findings.
3. Broader Market Factors: This study focuses primarily on LUNA and USTC. Expanding the analysis to include other cryptocurrencies and macroeconomic factors could enhance the understanding of how systemic risk propagates through the broader crypto ecosystem.

Building on this work, future studies could explore the role of sentiment analysis and news events in driving price crashes and recoveries. A broader analysis of other algorithmic stablecoins to assess commonalities and differences in their behavior during market crises would also be interesting. The development of predictive models for the early detection of liquidity crises in cryptocurrency markets also could be relevant.

Funding: This research received no external funding.

Institutional Review Board Statement: Not applicable.

Informed Consent Statement: Not applicable.

Data Availability Statement: The stablecoins and BTC data are freely available from Yahoo Finance! https://finance.yahoo.com/.

Acknowledgments: For their comments on earlier drafts, I wish to thank Julien CHEVALLIER, Bilel SANHAJI, Xingyuan Yao, Darko Vukovic, Frances Coppola, Luca Galati, Faten Ben Slimane, and conference participants at the Ghent Workshop on Fintech, the University of Ghent, Belgium, 2023.

Conflicts of Interest: The authors declare no conflicts of interest.

References

1. Briola, A.; Vidal-Tomás, D.; Wang, Y.; Aste, T. Anatomy of a Stablecoin's failure: The Terra-Luna case. *Financ. Res. Lett.* **2022**, *51*, 103358. [CrossRef]
2. Stanford, E. *Crypto Wars: Faked Deaths, Missing Billions and Industry Disruption*; Kogan Page Publishers: London, UK, 2021.
3. Lee, S.; Lee, J.; Lee, Y. Dissecting the Terra-LUNA crash: Evidence from the spillover effect and information flow. *Financ. Res. Lett.* **2022**, *53*, 103590. [CrossRef]
4. Liu, J.; Makarov, I.; Schoar, A. *Anatomy of a Run: The Terra Luna Crash*; Technical Report; National Bureau of Economic Research: Cambridge, MA, USA, 2023.
5. Bindseil, U.; Pantelopoulos, G. Unbacked Crypto-Assets, Stablecoins and CBDC. In *Introduction to Payments and Financial Market Infrastructures*; Springer: Berlin/Heidelberg, Germany, 2023; pp. 125–152.
6. Wong, R. Why Stablecoins Fail: An Economist's Post-Mortem on Terra. *Federal Reserve Bank of Richmond Economic Brief*. 2022. Available online: https://www.richmondfed.org/publications/research/economic_brief/2022/eb_22-24 (accessed on 18 September 2024).
7. Uhlig, H. *A Luna-Tic Stablecoin Crash*; Technical Report; National Bureau of Economic Research: Cambridge, MA, USA, 2022.
8. Anadu, K.; Azar, P.; Huang, C.; Cipriani, M.; Eisenbach, T.M.; La Spada, G.; Landoni, M.; Macchiavelli, M.; Malfroy-Camine, A.; Wang, J.C. Runs and Flights to Safety: Are Stablecoins the New Money Market Funds? 2023. Available online: https://papers.ssrn.com/sol3/papers.cfm?abstract_id=4594064 (accessed on 18 September 2024).
9. Quiroz-Gutierrez, M. Who is Do Kwon, the 'lunatic' who created a 60 billion dollars cryptocurrency that collapsed in days? *Fortune Crypto*. 2022 .
10. Ardizzi, G.; Bevilacqua, M.; Cerrato, E.; Di Iorio, A. Making it through the (crypto) winter: Facts, figures and policy issues. *Int. Econ./Econ. Internazionale* **2023**, *76*.
11. Kyosev, D.; Anastasovski, D.; Kikovic, M.; Voutyras, O. Terra luna and the future of internet investments: Towards a framework for investors' protections. *Preprints* **2022** . [CrossRef]
12. Doumenis, Y.; Izadi, J.; Dhamdhere, P.; Katsikas, E.; Koufopoulos, D. A critical analysis of volatility surprise in Bitcoin cryptocurrency and other financial assets. *Risks* **2021**, *9*, 207. [CrossRef]
13. Li, D.; Han, D.; Weng, T.H.; Zheng, Z.; Li, H.; Li, K.C. On Stablecoin: Ecosystem, architecture, mechanism and applicability as payment method. *Comput. Stand. Interfaces* **2024**, *87*, 103747. [CrossRef]
14. Ferretti, S.; Furini, M. On using twitter to understand the stablecoin terra collapse. In Proceedings of the 2023 ACM Conference on Information Technology for Social Good, Lisbon, Portugal, 6–8 September 2023; pp. 16–22.
15. Clements, R. Built to fail: The inherent fragility of algorithmic stablecoins. *Wake For. Law Rev. Online* **2021**, *11*, 131. [CrossRef]
16. Burke, M.E. From Tether to Terra: The Current Stablecoin Ecosystem and the Failure of Regulators. *Fordham J. Corp. Financ. Law* **2023**, *28*, 99.
17. Camacho, M. Vector smooth transition regression models for US GDP and the composite index of leading indicators. *J. Forecast.* **2004**, *23*, 173–196. [CrossRef]
18. Weise, C.L. The asymmetric effects of monetary policy: A nonlinear vector autoregression approach. *J. Money Credit. Bank.* **1999**, *31*, 85–108. [CrossRef]
19. Healy, J.D. A note on multivariate CUSUM procedures. *Technometrics* **1987**, *29*, 409–412. [CrossRef]
20. Nelson, C.R.; Plosser, C.R. Trends and random walks in macroeconmic time series: Some evidence and implications. *J. Monet. Econ.* **1982**, *10*, 139–162. [CrossRef]
21. Harvey, A.C. Trends and cycles in macroeconomic time series. *J. Bus. Econ. Stat.* **1985**, *3*, 216–227. [CrossRef]
22. Hunter, J.S. The exponentially weighted moving average. *J. Qual. Technol.* **1986**, *18*, 203–210. [CrossRef]
23. Tsang, W.W.H.; Chong, T.T.L. Profitability of the on-balance volume indicator. *Econ. Bull.* **2009**, *29*, 2424–2431.
24. Mitchell, D.; Białkowski, J.; Tompaidis, S. Volume-weighted average price tracking: A theoretical and empirical study. *IISE Trans.* **2020**, *52*, 864–889. [CrossRef]
25. Sherstinsky, A. Fundamentals of recurrent neural network (RNN) and long short-term memory (LSTM) network. *Phys. D Nonlinear Phenom.* **2020**, *404*, 132306. [CrossRef]
26. Chen, Y.; Hao, Y. A feature weighted support vector machine and K-nearest neighbor algorithm for stock market indices prediction. *Expert Syst. Appl.* **2017**, *80*, 340–355. [CrossRef]
27. Bacon, D.W.; Watts, D.G. Estimating the transition between two intersecting straight lines. *Biometrika* **1971**, *58*, 525–534. [CrossRef]
28. Anderson, H.M.; Vahid, F. Testing multiple equation systems for common nonlinear components. *J. Econom.* **1998**, *84*, 1–36. [CrossRef]

29. Luukkonen, R.; Saikkonen, P.; Teräsvirta, T. Testing linearity against smooth transition autoregressive models. *Biometrika* **1988**, *75*, 491–499. [CrossRef]
30. Teräsvirta, T.; Yang, Y. *Linearity and Misspecification Tests for Vector Smooth Transition Regression Models*; Technical Report; CREATES Research Paper 2014-4; School of Economics and Management: Copenhagen, Denmark, 2014.